

Article

Tomonaga–Luttinger Spin Liquid and Kosterlitz–Thouless Transition in the Spin-1/2 Branched Chains: The Study of Topological Phase Transition

Hamid Arian Zad ^{1,2,*} , Azam Zoshki ² , Nerses Ananikian ^{1,3}  and Michal Jaščur ² ¹ Alikhanyan National Science Laboratory, Alikhanian Br. 2, Yerevan 0036, Armenia; ananik@yerphi.am² Department of Theoretical Physics and Astrophysics, Faculty of Science, P. J. Šafárik University, Park Angelinum 9, 041 54 Kosice, Slovakia; zoshkia@yahoo.com (A.Z.); michal.jascgur@upjs.sk (M.J.)³ CANDLE Synchrotron Research Institute, Acharyan 31, Yerevan 0022, Armenia

* Correspondence: arianzad.hamid@yerphi.am

Abstract: In the present work, we provide a comprehensive numerical investigation of the magnetic properties and phase spectra of three types of spin-1/2 branched chains consisting of one, two and three side spins per unit block with intra-chain interaction and a uniform inter-chain interaction in the presence of an external magnetic field. In a specific magnetic field interval, the low-temperature magnetization of these chains shows a step-like behavior with a pronounced plateau depending on the strength and the type of intra-chain interaction being ferromagnetic or antiferromagnetic. We demonstrate that when inter-chain interaction J_1 is antiferromagnetic and intra-chain interaction J_2 is ferromagnetic, the magnetization of the models manifests a smooth increase without a plateau, which is evidence of the existence of a Luttinger-like spin liquid phase before reaching its saturation value. On the other hand, when J_1 is ferromagnetic and J_2 is antiferromagnetic, the low-temperature magnetization of the chain with two branches shows an intermediate plateau at one-half of the saturation magnetization that breaks a quantum spin liquid phase into two regions. The magnetization of the chain with three branches exhibits two intermediate plateaus and two regions of a quantum spin liquid. We demonstrate that the chains with more than one side spin illustrate in their ground-state phase diagram a Kosterlitz–Thouless transition from a gapful phase to a gapless spin liquid phase.

Keywords: magnetization; intra-chain interaction; spin liquid phase; Kosterlitz–Thouless transition



Citation: Arian Zad, H.; Zoshki, A.; Ananikian, N.; Jaščur, M. Tomonaga–Luttinger Spin Liquid and Kosterlitz–Thouless Transition in the Spin-1/2 Branched Chains: The Study of Topological Phase Transition. *Materials* **2022**, *15*, 4183. <https://doi.org/10.3390/ma15124183>

Academic Editors: Haiou Wang and Dexin Yang

Received: 22 April 2022

Accepted: 9 June 2022

Published: 13 June 2022

Publisher's Note: MDPI stays neutral with regard to jurisdictional claims in published maps and institutional affiliations.



Copyright: © 2022 by the authors. Licensee MDPI, Basel, Switzerland. This article is an open access article distributed under the terms and conditions of the Creative Commons Attribution (CC BY) license (<https://creativecommons.org/licenses/by/4.0/>).

1. Introduction

Throughout the years, Heisenberg spin models have been considered as usual tools to characterize the destiny of a material in different circumstances [1–7]. For example, in references [8–11], the absence of long-range order was proved in the presence of an exchange interaction for 1-D and 2-D quantum Heisenberg systems. Magnetic properties of metals introduced in terms of spin models have attracted intense interest from researchers due to their potential implementations in condensed matter physics and materials science [12–18].

During the recent decades, substantial advances in designing single-chain magnets (SCMs) [19–22] have come to pass by means of 1-D quantum spin models. For the time being, heterometallic SCMs are important quantum ferrimagnetic chains for physical realizations of metal-containing polymers. They have already attracted a great deal of attention from chemists and physicists due to the fact that they exhibit a lot of unconventional magnetic properties at low temperatures. The main reason behind particular magnetic behavior is the interplay between ferromagnetic and antiferromagnetic spin states [23–25].

The magnetization of 1-D Heisenberg chain models reveals fascinating features such as an intermediate plateau [17,18,26–36], jumps and steps [37–40], and spin liquid states [24,25,41,42]. In recent works, the ground-state phase diagram and the low-temperature magnetization process of several spin-1/2 Heisenberg branched chains have been examined, whose magnetic structure is inspired by the heterobimetallic coordination polymers [43,44]. In

reference [45], the ground-state phase transition and magnetic properties of a frustrated spin chain with side chains have been investigated in detail. Motivated by novel, highly correlated low-dimensional systems, V. O. Chervanovskii et al. studied the magnetization process of a series of spin-1/2 chains with different types of intra-chain interactions at low temperatures [46]. The Kondo-necklace models with similar spin structure to the branched chains were considered, and some important results for their ground-state phase transition have been reported [47,48].

Despite the fact that linear spin chains with side spins comprise a rich physics in materials science and technology, less attention has been paid to the effect of the number of branches, to the nature of interactions between chain and side spins, and to the effect of intra-chain interactions on the ground-state phase spectra of these models. In the present paper, we will numerically discuss the low-temperature magnetic properties of the spin-1/2 XXX Heisenberg model on the three different branched chains with one, two and three intra-chain interactions in their unit blocks. Hereafter, we label these chains as chain Y_1 , chain Y_2 and chain Y_3 , respectively. In fact, we will widely discuss the problem concerning the effects of side spins and their exchange interaction on the ground-state phase spectra and the magnetization process of the above-described spin-1/2 Heisenberg branched chains. To gain a reasonable insight into the low-temperature magnetization process of the chain models, we use Quantum Monte Carlo (QMC) simulations under the subroutine dirloop-sse—a package from the Algorithms and Libraries for Physics Simulations (ALPS) project, which prepares a full generic implementation of the QMC simulations for spin lattices [49,50].

The paper is organized as follows. In Section 2, the spin-1/2 XXX Heisenberg model on the three different types of 1-D branched chains with one, two and three intra-chain interactions per unit cell is introduced. In Section 3, we numerically investigate the magnetic properties of the introduced spin chains by implementing QMC simulations. The following input parameters are considered for the applied sse loop: 1×10^5 thermalization, 1×10^4 MC sweeps, assuming periodic boundary conditions. Next, we report the most interesting results obtained for the magnetic behavior of the spin chains Y_1, Y_2 and Y_3 under two different conditions considered for the nature of inter- and intra-chain interactions J_1 and J_2 . In particular, the effect of the intra-chain interaction J_2 between side spins and chains on the low-temperature magnetization of the introduced models will be discussed in detail. The conclusions are drawn in Section 4.

2. The Model

Let us consider the spin-1/2 XXX Heisenberg model on the branched chains illustrated in Figure 1 described by an effective Hamiltonian

$$\mathcal{H} = \sum_{i=1}^N \left\{ J_1 (\mathbf{S}_{A_i} \cdot \mathbf{S}_{B_i} + \mathbf{S}_{B_i} \cdot \mathbf{S}_{A_{i+1}}) + \sum_{j=1}^n [J_2 (\mathbf{S}_{A_i} \cdot \mathbf{S}_{C_{ij}})] - g\mu_B H (\mathbf{S}_{A_i}^z + \mathbf{S}_{B_i}^z + \mathbf{S}_{C_{ij}}^z) \right\} \quad (1)$$

where N is the number of unit cells, and n accounts for the number of side spins. The total number of spins $L = (n + 2)N$ is considered for the systems under periodic boundary conditions, where $\mathbf{S}_{A_{N+1}} \equiv \mathbf{S}_{A_1}$. J_1 and J_2 are, respectively, inter- and intra-chain exchange interactions between each of the two nearest neighbor spins, H is the applied magnetic field in the z -direction. g and μ_B are g -factor and Bohr magneton, respectively. The XXX interaction between each pair of spins can be formulated as

$$\mathbf{S}_\alpha \cdot \mathbf{S}_{\alpha'} = S_\alpha^x S_{\alpha'}^x + S_\alpha^y S_{\alpha'}^y + S_\alpha^z S_{\alpha'}^z \quad (2)$$

in which spin-1/2 operators are given by ($\hbar = 1$)

$$s^x = \frac{1}{2} \begin{pmatrix} 0 & 1 \\ 1 & 0 \end{pmatrix}, \quad s^y = \frac{1}{2} \begin{pmatrix} 0 & -i \\ i & 0 \end{pmatrix}, \quad s^z = \frac{1}{2} \begin{pmatrix} 1 & 0 \\ 0 & -1 \end{pmatrix} \quad (3)$$

Henceforward, to have a dimensionless parameter space, in our numerical tasks, the intra-chain exchange interaction J_2 will be considered as the energy unit.

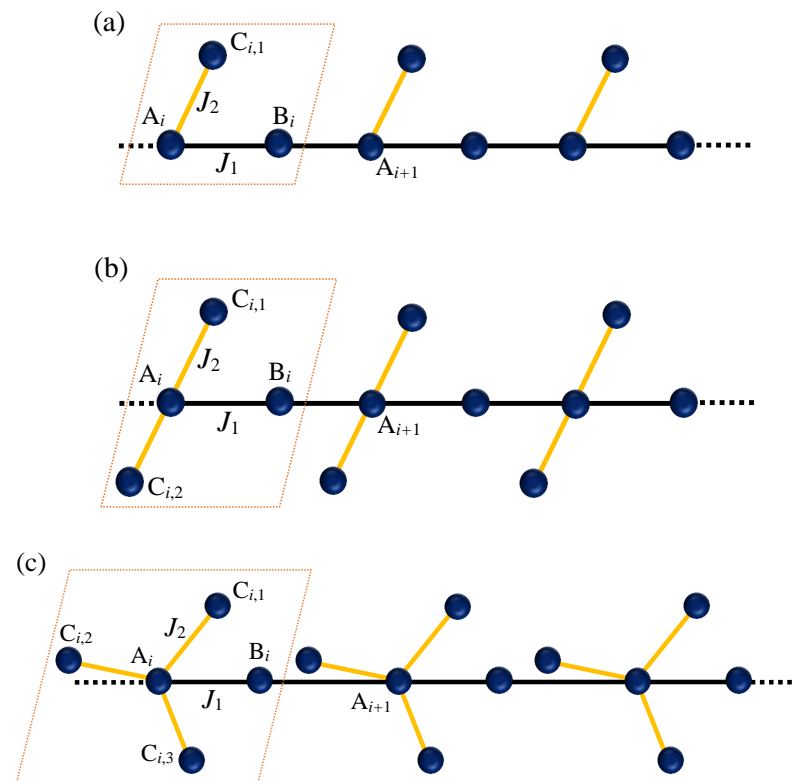


Figure 1. Schematic structure of the spin-1/2 XXX Heisenberg model on the branched chains (a) Y_1 with one, (b) Y_2 with two, and (c) Y_3 with three intra-chain interactions J_2 . J_1 denotes inter-chain interaction. In each case, the dotted rectangle indicates a unit cell that uniformly repeats throughout the chains. Solid balls labeled as A, B, and C represent spin-1/2 particles in a unit block, and the balls marked with C_i indicate the side spins.

3. Magnetic Properties

To demonstrate the magnetic properties of the three types of 1-D spin-1/2 Heisenberg branched chains Y_{1-3} , we have calculated the low-temperature magnetization process using the QMC method with the stochastic series expansion implementation from the ALPS package with $L = 120$ number of spins. Two following conditions are supposed for the exchange couplings J_1 and J_2 :

- ❖ Condition (I): We assume ferromagnetic coupling $|J_2|$ is the energy unit ($J_2 < 0$) where the magnetization of the models is examined for different antiferromagnetic interaction ratios $J_1/|J_2| > 0$.
- ❖ Condition (II): We assume antiferromagnetic coupling $J_2 > 0$ is the energy unit, and the magnetization is investigated for various fixed values of the ferromagnetic interaction ratio $J_1/J_2 < 0$.

The main goal of the above selection of antiferromagnetic–ferromagnetic interactions is to study the competition between antiferromagnetism and ferromagnetism to determine the predomination of the gapless spin liquid phases and to detect the Kosterlitz–Thouless (KT) critical point in the ground-state phase spectra of the models.

3.1. The Heisenberg Spin-1/2 Branched Chains under Condition (I)

Figure 2 displays QMC simulations of the magnetization per saturation value M/M_s for the chains Y_{1-3} versus the magnetic field at low enough temperature $k_B T/|J_2| = 0.02$ (T is the temperature and k_B is the Boltzmann constant).

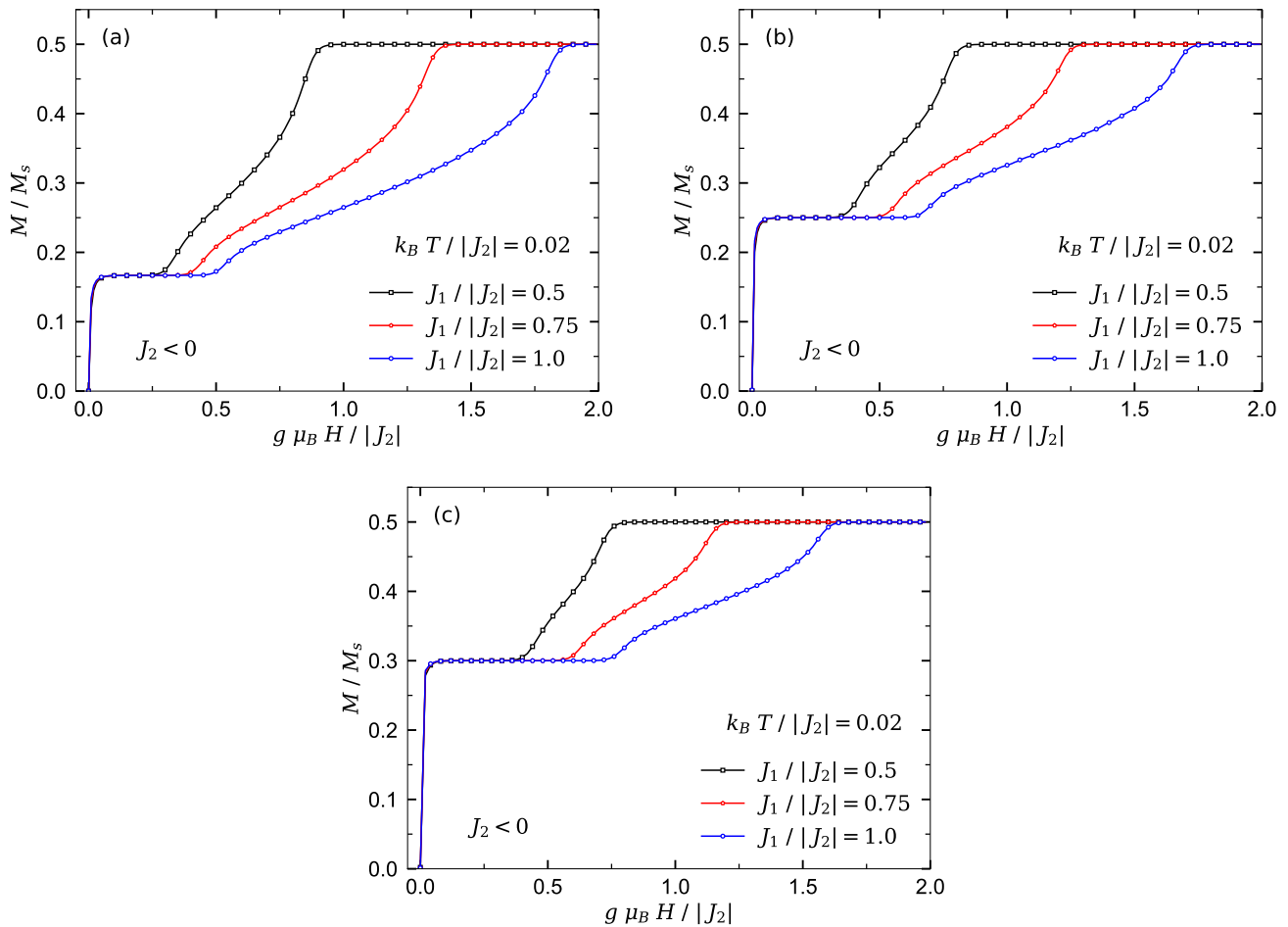


Figure 2. QMC results obtained for the magnetization curve of the three Heisenberg branched chains at low temperatures $k_B T/|J_2| = 0.02$ under the condition (I) where three different fixed values of the inter-chain interaction $J_1/|J_2| = \{0.5, 0.75, 1.0\}$ are considered. (a) The magnetization of chain Y_1 . (b) The magnetization of chain Y_2 . (c) The magnetization of chain Y_3 .

As can be seen in Figure 2, the magnetization of each spin chain shows an abrupt jump when the magnetic field increases from zero. This quantity reaches an intermediate magnetization plateau at the fractional value $M/M_s = n/(n+2)$. This single plateau coincides with the gapful Lieb–Mattis (LM) ferrimagnetic ground state [25,51]. Obviously, increasing the number of side spins n results in enhancing the height and width of LM plateau. The intermediate plateau terminates at a critical magnetic field due to a quantum phase transition to a Luttinger spin liquid phase. Evidently, increasing the interaction ratio $J_1/|J_2|$ enhances the region of the spin liquid phase, as well as the saturation field, while increasing the number of side spins restricts the region of the spin liquid phase and decreases the saturation field (compare Figure 2a with Figure 2b,c).

3.2. The Heisenberg Spin-1/2 Branched Chains under Condition (II)

The spin chains Y_2 and Y_3 show more interesting magnetic properties under the condition (II). To shed light on this issue, we plot the magnetization curve of models Y_{1-3} versus the magnetic field at $k_B T / J_2 = 0.02$, where a few selected values of the interaction ratio J_1 / J_2 are supposed. The model Y_1 displays in its magnetization process a single intermediate plateau at one-third of the saturation magnetization (see Figure 3a). When the interaction ratio J_1 / J_2 becomes ferromagnetically stronger, a spin liquid phase emerges into the ground-state phase spectra of this model.

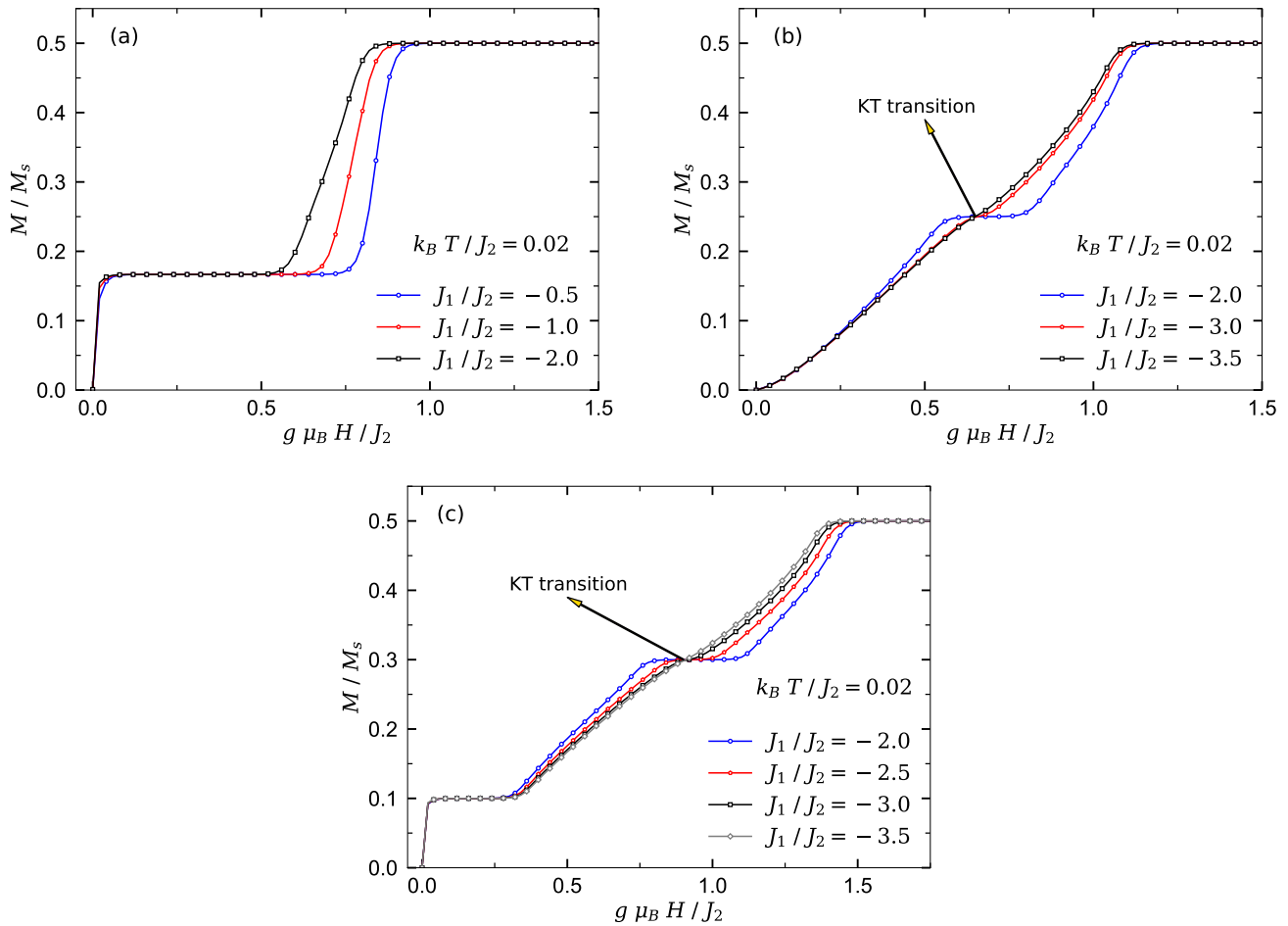


Figure 3. QMC results obtained for the magnetization curve of the three Heisenberg branched chains at low temperatures $k_B T / J_2 = 0.02$ under the condition (II), assuming a few fixed values of the inter-chain interaction J_1 / J_2 . (a) Chain Y_1 . (b) Chain Y_2 . (c) Chain Y_3 .

By inspecting Figure 3b, we realize that except for the case shown in Figure 2b, the magnetization of the model Y_2 under condition (II) shows a wide spin liquid phase at low magnetic fields instead of the LM ferrimagnetic phase. An intermediate magnetization plateau at one-half of the saturation value appears at moderate magnetic fields. We find that this intermediate magnetization plateau terminates at a quantum KT critical point when the absolute value of interaction ratio J_1 / J_2 increases.

The sharp decrease in the susceptibility χ of chain Y_2 (see Figure 4a) nearby the relevant quantum critical point $g \mu_B H / J_2 \approx 0.65$ is solid evidence of the KT transition.

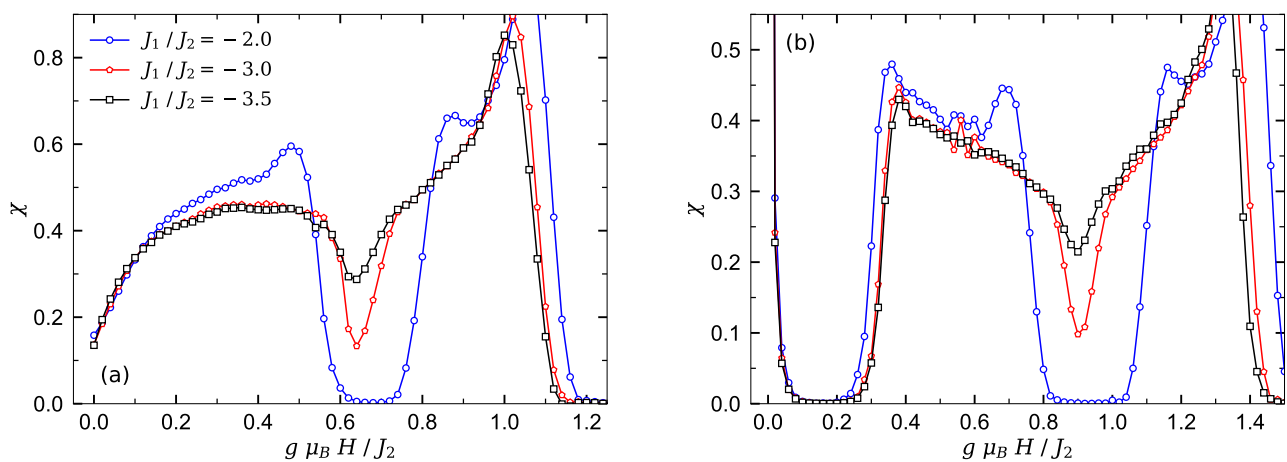


Figure 4. The low-temperature susceptibility χ versus magnetic field for (a) the Heisenberg branched chain Y_2 and (b) chain Y_3 , at $k_B T / J_2 = 0.02$ under the condition (II). Three different values of the inter-chain interaction $J_1 / J_2 = \{-2.0, -3.0, -3.5\}$ are considered for the both panels.

When the number of side spins increases, the branched chain illustrates different magnetization behavior at low temperature. For instance, in Figure 3c, the magnetization of chain Y_3 is presented for different fixed values of the interaction ratio J_1 / J_2 . It is quite obvious that the magnetization of model Y_3 manifests two intermediate plateaus at one-fifth and three-fifth of the saturation magnetization. In fact, by increasing the magnetic field from zero, the magnetization abruptly jumps to the first intermediate plateau. This quantity starts to increase smoothly from the first plateau at a critical magnetic field ($g\mu_B H / J_2 \approx 0.3$) and reaches the second intermediate plateau, and successively a second smooth increase of the magnetization starts from another critical magnetic field nearby $g\mu_B H / J_2 \approx 1.1$. These smooth increases of the magnetization are reminiscent of the existence of the Tomonaga–Luttinger spin liquid in the ground-state phase diagram of chain Y_3 . It can be seen from Figure 3c that the second intermediate plateau ($M / M_s = 3/5$) appeared in the magnetization curve of the branched chain Y_3 monotonically shrinks upon increasing the interaction ratio J_1 / J_2 . This plateau eventually disappears at a quantum critical KT point $g\mu_B H / J_2 \approx 0.9$. The steep decrease in the susceptibility χ shown in Figure 4b close to this point denotes a quantum KT transition. Clearly, magnetic susceptibility χ vanishes for the gapful phases, while it has unconventional behavior with nonzero value within the gapless spin liquid phase regions.

4. Conclusions

To summarize, we have numerically investigated the magnetic properties of the spin-1/2 XXX Heisenberg model on the three different 1-D branched chains consisting of one, two and three intra-chain interactions per unit cell. Indeed, we have examined the magnetization and magnetic susceptibility of these spin systems by employing the QMC method.

When the intra-chain interaction is ferromagnetic and inter-chain interaction is antiferromagnetic, the magnetization of all chains shows a single intermediate plateau whose height is related to the number of side spins. This plateau terminates at a critical field, and successively, a gapless Tomonaga–Luttinger liquid phase arises, where the magnetization starts to increase smoothly until it reaches its saturation value. We understood that by increasing the number of side spins, the phase region corresponds to the Luttinger liquid phase diminishes.

On the other hand, when the intra-chain interaction is antiferromagnetic and inter-chain interaction is ferromagnetic, the low-temperature magnetization of the branched chains with more than one side spin per unit cell exhibit more rich magnetic properties. Under this situation, the magnetization of the branched chain with two side spins shows

an intermediate plateau at one-half of saturation value that breaks the quantum spin liquid into two areas. We have concluded that for a relatively strong value of the ferromagnetic inter-chain interaction this plateau terminates at a quantum KT critical point.

Moreover, we have observed that the magnetization of chain with three side spins shows two intermediate plateaus at one-fifth and three-fifth of the saturation magnetization. Another interesting finding from our investigations is that with an increase in the inter-chain interaction, the intermediate plateau at three-fifth of saturation magnetization gradually shrinks and eventually ends up at a KT point, while the intermediate plateau at one-fifth of saturation magnetization becomes more robust.

We theoretically concluded that the considered Heisenberg branched chains reveal an interesting magnetic response to the quantity and quality of the intra-chain interaction. It is expected that our results could be useful for explaining the magnetic behavior of various metal-containing polymers with different side spins.

Author Contributions: Data curation, H.A.Z.; Formal analysis, A.Z.; Investigation, H.A.Z. and N.A.; Methodology, A.Z.; Project administration, H.A.Z.; Resources, A.Z.; Software, H.A.Z. and A.Z.; Supervision, N.A. and M.J.; Validation, M.J.; Visualization, A.Z.; Writing—original draft, H.A.Z.; Writing—review and editing, H.A.Z., A.Z. and M.J. All authors have read and agreed to the published version of the manuscript.

Funding: This work was supported by the SAIA (Slovak Academic Information Agency), and Ministry of Education, Science, Research and Sport of the Slovak Republic under contract No. VEGA 1/0531/19 and the Slovak Research and Development Agency provided under Contract No. APVV-20-0150.

Acknowledgments: H. Arian Zad and A. Zoshki acknowledge the financial support of the National Scholarship Programme of the Slovak Republic (NŠP). H. Arian Zad also acknowledges the receipt of the grant from the Abdus Salam International Centre for Theoretical Physics (ICTP), Trieste, Italy. N. Ananikian acknowledges the support of CS MES RA in the frame of the research project No. SCS 19IT-008 and research project No. SCS 21AG-1C006. M. Jaščur has been supported by the Grant of Ministry of Education, Science, Research and Sport of the Slovak Republic under contract No. VEGA 1/0531/19, and Grant of the Slovak Research and Development Agency provided under Contract No. APVV-20-0150.

Conflicts of Interest: The authors declare no conflict of interest.

References

1. Kuramoto, T. Magnetic and Critical Properties of Alternating Spin Heisenberg Chain in a Magnetic Field. *J. Phys. Soc. Jpn.* **1998**, *67*, 1762. [[CrossRef](#)]
2. Yamamoto, S.; Sakai, T. Breakdown of a magnetization plateau due to anisotropy in Heisenberg mixed-spin chains. *J. Phys. Condens. Matter* **1999**, *11*, 5175. [[CrossRef](#)]
3. Sakai, T.; Yamamoto, S. Critical behavior of anisotropic Heisenberg mixed-spin chains in a field. *Phys. Rev. B* **1999**, *60*, 4053. [[CrossRef](#)]
4. Ivanov, N.B. Magnon dispersions in quantum Heisenberg ferrimagnetic chains at zero temperature. *Phys. Rev. B* **2000**, *62*, 3271. [[CrossRef](#)]
5. Rojas, M.; Rojas, O.; de Souza, S.M. Frustrated Ising model on the Cairo pentagonal lattice. *Phys. Rev. E* **2012**, *86*, 051116. [[CrossRef](#)] [[PubMed](#)]
6. Rousochatzakis, I.; Läuchli, A.M.; Moessner, R. Quantum magnetism on the Cairo pentagonal lattice. *Phys. Rev. B* **2012**, *85*, 104415. [[CrossRef](#)]
7. Rodrigues, F.C.; de Souza, S.M.; Rojas, O. Geometrically frustrated Cairo pentagonal lattice stripe with Ising and Heisenberg exchange interactions. *Ann. Phys.* **2017**, *379*, 1. [[CrossRef](#)]
8. Mermin, N.D.; Wagner, H. Absence of Ferromagnetism or Antiferromagnetism in One- or Two-Dimensional Isotropic Heisenberg Models. *Phys. Rev. Lett.* **1966**, *17*, 1133. [[CrossRef](#)]
9. Halperin, B.E. On the Hohenberg–Mermin–Wagner Theorem and Its Limitations. *J. Stat. Phys.* **2018**, *175*, 521. [[CrossRef](#)]
10. Hohenberg, P.C. Existence of Long-Range Order in One and Two Dimensions. *Phys. Rev.* **1967**, *158*, 383. [[CrossRef](#)]
11. Zivieri, R. Absence of Spontaneous Spin Symmetry Breaking in 1D and 2D Quantum Ferromagnetic Systems with Bilinear and Biquadratic Exchange Interactions. *Symmetry* **2020**, *12*, 2061. [[CrossRef](#)]
12. Bonner, J.C.; Fisher, M.E. Linear Magnetic Chains with Anisotropic Coupling. *Phys. Rev.* **1964**, *135*, A640. [[CrossRef](#)]
13. Carlin, R.L. *Magnetochemistry*; Springer: Dordrecht, The Netherlands, 1986.

14. Kahn, O. *Molecular Magnetism*, 1st ed.; Wiley-VCH: New York, NY, USA, 1993.
15. Torrico, J.; Ohanyan, V.; Rojas, O. Non-conserved magnetization operator and ‘fire-and-ice’ ground states in the Ising-Heisenberg diamond chain. *J. Magn. Magn. Mater.* **2018**, *454*, 85–96. [[CrossRef](#)]
16. Chen, W.P.; Singleton, J.; Qin, L.; Camón, A.; Engelhardt, L.; Luis, F.; Winpenny, R.E.; Zheng, Y.Z. Quantum Monte Carlo simulations of a giant $\{\text{Ni}_{21}\text{Gd}_{20}\}$ cage with a $S=91$ spin ground state. *Nat. Comm.* **2018**, *9*, 2107. [[CrossRef](#)] [[PubMed](#)]
17. Eggert, S.; Affleck, I.; Takahashi, M. Susceptibility of the spin $1/2$ Heisenberg antiferromagnetic chain. *Phys. Rev. Lett.* **1994**, *73*, 332. [[CrossRef](#)] [[PubMed](#)]
18. Eggert, S. Accurate determination of the exchange constant in Sr_2CuO_3 from recent theoretical results. *Phys. Rev. B* **1996**, *53*, 5116. [[CrossRef](#)] [[PubMed](#)]
19. Pardo, E.; Ruiz-García, R.; Lloret, F.; Faus, J.; Julve, M.; Journaux, Y.; Delgado, F.; Ruiz-Peréz, C. Cobalt(II)–Copper(II) Bimetallic Chains as a New Class of Single-Chain Magnets. *Adv. Mater.* **2004**, *16*, 1597. [[CrossRef](#)]
20. Choi, S.W.; Kwak, H.Y.; Yoon, J.H.; Kim, H.C.; Koh, E.K.; Hong, C.S. Intermolecular Contact-Tuned Magnetic Nature in One-Dimensional 3d–5d Bimetallic Systems: From a Metamagnet to a Single-Chain Magnet. *Inorg. Chem.* **2008**, *47*, 10214. [[CrossRef](#)]
21. Yamamoto, S. Magnetic Properties of Quantum Ferrimagnetic Spin Chains. *Phys. Rev. B* **1999**, *59*, 1024. [[CrossRef](#)]
22. Sakai, T.; Yamamoto, S. Quantum magnetization plateaus in ferrimagnetic spin chains. *J. Magn. Magn. Mater.* **2001**, *226*, 645. [[CrossRef](#)]
23. Strečka, J.; Verkholyak, T. Magnetic Signatures of Quantum Critical Points of the Ferrimagnetic Mixed Spin- $(1/2, S)$ Heisenberg Chains at Finite Temperatures. *J. Low Temp. Phys.* **2017**, *187*, 712. [[CrossRef](#)]
24. Veríssimo, L.M.; Pereira, M.S.S.; Strečka, J.; Lyra, M.L. Kosterlitz-Thouless and Gaussian criticalities in a mixed spin- $(\frac{1}{2}, \frac{5}{2}, \frac{1}{2})$ Heisenberg branched chain with exchange anisotropy. *Phys. Rev. B* **2019**, *99*, 134408. [[CrossRef](#)]
25. Strečka, J. Breakdown of a Magnetization Plateau in Ferrimagnetic Mixed Spin- $(1/2, S)$ Heisenberg Chains due to a Quantum Phase Transition towards the Luttinger Spin Liquid. *Act. Phys. Pol. A* **2017**, *131*, 624. [[CrossRef](#)]
26. Motoyama, N.; Eisaki, H.; Uchida, S. Magnetic Susceptibility of Ideal Spin $1/2$ Heisenberg Antiferromagnetic Chain Systems, Sr_2CuO_3 and SrCuO_2 . *Phys. Rev. Lett.* **1996**, *76*, 3212. [[CrossRef](#)] [[PubMed](#)]
27. Oshikawa, M.; Ueda, K.; Aoki, H.; Ochiai, A.; Kohgi, M. Field-Induced Gap Formation in Yb_4As_3 . *J. Phys. Soc. Jpn.* **1999**, *68*, 3181. [[CrossRef](#)]
28. Oshikawa, M.; Affleck, I. Field-Induced Gap in $S = 1/2$ Antiferromagnetic Chains. *Phys. Rev. Lett.* **1997**, *79*, 2883. [[CrossRef](#)]
29. Kikuchi, H.; Fujii, Y.; Chiba, M.; Mitsudo, S.; Idehara, T.; Tonegawa, T.; Okamoto, K.; Sakai, T.; Kuwai, T.; Ohta, H. Experimental observation of the $1/3$ magnetization plateau in the diamond-chain compound $\text{Cu}_3(\text{CO}_3)_2(\text{OH})_2$. *Phys. Rev. Lett.* **2005**, *94*, 227201. [[CrossRef](#)]
30. Hida, K. Magnetic Properties of the Spin- $1/2$ Ferromagnetic-Ferromagnetic-Antiferromagnetic Trimerized Heisenberg Chain. *J. Phys. Soc. Jpn.* **1994**, *63*, 2359–2364. [[CrossRef](#)]
31. Oshikawa, M.; Yamanaka, M.; Affleck, I. Magnetization Plateaus in Spin Chains: “Haldane Gap” for Half-Integer Spins. *Phys. Rev. Lett.* **1997**, *78*, 1984. [[CrossRef](#)]
32. Leiner, J.C.; Oh, J.; Kolesnikov, A.I.; Stone, M.B.; Le, M.D.; Kenny, E.P.; Powell, B.J.; Mourigal, M.; Gordon, E.E.; Whangbo, M.-H.; et al. Magnetic excitations of the Cu^{2+} quantum spin chain in $\text{Sr}_3\text{CuPtO}_6$. *Phys. Rev. B* **2018**, *97*, 104426. [[CrossRef](#)]
33. Arian Zad, H.; Ananikian, N. Phase transitions and magnetization of the mixed-spin Ising-Heisenberg double sawtooth frustrated ladder. *J. Phys. Condens. Matter.* **2017**, *29*, 455402. [[CrossRef](#)]
34. Arian Zad, H.; Ananikian, N.; Jaščur, M. Single-ion anisotropy effects on the demagnetization process of the alternating weak-rung interacting mixed spin- $(1/2, 1)$ Ising-Heisenberg double saw-tooth ladders. *Phys. Scr.* **2020**, *95*, 095702. [[CrossRef](#)]
35. Arian Zad, H.; Trombettoni, A.; Ananikian, N. Spin- $1/2$ Ising–Heisenberg Cairo pentagonal model in the presence of an external magnetic field: Effect of Landé g -factors. *Eur. Phys. J. B* **2020**, *93*, 200. [[CrossRef](#)]
36. Arian Zad, H.; Kenna, R.; Ananikian, N. Magnetic and thermodynamic properties of the octanuclear nickel phosphonate-based cage. *Phys. A* **2020**, *538*, 122841. [[CrossRef](#)]
37. Strečka, J.; Karľová, K.; Madaras, T. Giant magnetocaloric effect, magnetization plateaus and jumps of the regular Ising polyhedra. *Phys. B* **2015**, *466–467*, 76–85. [[CrossRef](#)]
38. Gálisová, L.; Strečka, J. Magnetic and magnetocaloric properties of the exactly solvable mixed-spin Ising model on a decorated triangular lattice in a magnetic field. *Phys. E* **2018**, *99*, 244. [[CrossRef](#)]
39. Strečka, J.; Richter, J.; Derzhko, O.; Verkholyak, T.; Karľová, K. Magnetization process and low-temperature thermodynamics of a spin- $1/2$ Heisenberg octahedral chain. *Phys. B* **2018**, *536*, 364. [[CrossRef](#)]
40. Strečka, J.; Karľová, K.; Baliha, V.; Derzhko, O. Ising versus Potts criticality in low-temperature magnetothermodynamics of a frustrated spin- $\frac{1}{2}$ Heisenberg triangular bilayer. *Phys. Rev. B* **2018**, *98*, 174426. [[CrossRef](#)]
41. Balents, L. Spin liquids in frustrated magnets. *Nature* **2010**, *464*, 199. [[CrossRef](#)] [[PubMed](#)]
42. Savary, L.; Balents, L. Quantum spin liquids: A review. *Rep. Prog. Phys.* **2017**, *80*, 016502. [[CrossRef](#)] [[PubMed](#)]
43. Karľová, K.; Strečka, J.; Lyra, M.L. Breakdown of intermediate one-half magnetization plateau of spin- $1/2$ Ising-Heisenberg and Heisenberg branched chains at triple and Kosterlitz-Thouless critical points. *Phys. Rev. E* **2019**, *100*, 042127. [[CrossRef](#)] [[PubMed](#)]
44. Jiang, J.J. Ground-state properties of a quantum frustrated spin chain with side spins and arbitrary spin s . *J. Mag. Magn. Mat.* **2021**, *539*, 168392. [[CrossRef](#)]

45. Takano, K.; Hida, K. Disordered ground states in a quantum frustrated spin chain with side chains. *Phys. Rev. B* **2008**, *77*, 134412. [[CrossRef](#)]
46. Cheranovskii, V.O.; Slavin, V.V.; Klein, D.J. Quantum phase transitions in frustrated 1D Heisenberg spin systems. *Low Temp. Phys.* **2021**, *47*, 443. [[CrossRef](#)]
47. Essler, F.H.L.; Kuzmenko, T. Luttinger liquid coupled to quantum spins: Flow equation approach to the Kondo necklace model. *Phys. Rev. B* **2007**, *76*, 115108. [[CrossRef](#)]
48. Hemmatiyan, S.; Movassagh, M.R.; Ghassemi, N.; Kargarian, M.; Rezakhani, A.T.; Langari, A. Quantum phase transitions in the Kondo-necklace model: Perturbative continuous unitary transformation approach. *J. Phys. Condens. Matter* **2015**, *27*, 155601. [[CrossRef](#)]
49. Bauer, B.; Carr, L.D.; Evertz, H.G.; Feiguin, A.; Freire, J.; Fuchs, S.; Gamper, L.; Gukelberger, J.; Gull, E.; Guertler, S.; et al. The ALPS project release 2.0: Open source software for strongly correlated systems. *J. Stat. Mech.* **2011**, P05001. [[CrossRef](#)]
50. Albuquerque, A.F.; Alet, F.; Corboz, P.; Dayal, P.; Feiguin, A.; Fuchs, S.; Gamper, L.; Gull, E.; Gürtler, S.; Honecker, A.; et al. The ALPS project release 1.3: Open-source software for strongly correlated systems. *J. Magn. Magn. Mater.* **2007**, *310*, 1187. [[CrossRef](#)]
51. Lieb, E.; Mattis, D. Ordering Energy Levels of Interacting Spin Systems. *J. Math. Phys.* **1962**, *3*, 749. [[CrossRef](#)]